Development of a quartz tuning-fork-based force sensor for measurements in the tens of nanoNewton force range during nanomanipulation experiments

V. T. A. Oiko,[1,a)] B. V. C. Martins,[2] P. C. Silva,[3] V. Rodrigues,[1] and D. Ugarte[1]
[1]*Instituto de Física "Gleb Wataghin," Univ. Estadual de Campinas (UNICAMP), Campinas 13083-859, Brazil*
[2]*Department of Physics, University of Alberta, Edmonton, Alberta T6G 2R3, Canada*
[3]*Laboratório Nacional de Nanotecnologia, CNPEM, Campinas 13083-970, Brazil*

(Received 22 November 2013; accepted 26 February 2014; published online 17 March 2014)

Understanding the mechanical properties of nanoscale systems requires new experimental and theoretical tools. In particular, force sensors compatible with nanomechanical testing experiments and with sensitivity in the nN range are required. Here, we report the development and testing of a tuning-fork-based force sensor for *in situ* nanomanipulation experiments inside a scanning electron microscope. The sensor uses a very simple design for the electronics and it allows the direct and quantitative force measurement in the 1–100 nN force range. The sensor response is initially calibrated against a nN range force standard, as, for example, a calibrated Atomic Force Microscopy cantilever; subsequently, applied force values can be directly derived using only the electric signals generated by the tuning fork. Using a homemade nanomanipulator, the quantitative force sensor has been used to analyze the mechanical deformation of multi-walled carbon nanotube bundles, where we analyzed forces in the 5–40 nN range, measured with an error bar of a few nN. © *2014 AIP Publishing LLC*. [http://dx.doi.org/10.1063/1.4868236]

I. INTRODUCTION

The advent of nanotechnology has raised the demand of novel tools and techniques pushing instruments and methods to astonishing performances. When dealing with the tiny nano-objects, simple laboratory procedures may become technical or scientific challenges, whose solutions are not usually straightforward. This has led the scientific society to organize national or international priority initiatives, which induced huge technical efforts on the development of instrumentation suitable for nanosystem studies. Among experimental challenges, the analysis of the mechanical response in nanoscale materials and the understanding of the physical basis of friction have been particularly emphasized.[1]

As the analysis of nanomaterials requires high spatial resolution capabilities, many experiments addressing mechanical properties have been performed using Atomic Force Microscopy (AFM) and silicon cantilevers. In addition, the development of AFM dynamic modes (e.g., Frequency Modulation, FM-AFM and Amplitude Modulation, AM-AFM) allowed this imaging approach to become very versatile, fast, and easy to apply. In fact, during nanomechanical experiments, the cantilever has been employed for both, imaging and mechanical probing.[2–4] However, we must keep in mind that the very popular FM methodology just provides the force's gradient and it does not allow the direct force measurement.[5] In these cases, the force is usually determined by applying basically the Hooke's law.[5–11] On the other hand, amplitude modulation also allows direct force sensing and the assessment of mechanical properties of a variety of materials.[6] Recently, quartz tuning forks (TF) have also been characterized[12,13] and optimized as AFM force sensors for imaging using both AM and FM[12,14–17] and for the mechanical characterization.[7,18–20]

The huge potential of micro and nanoscale devices has raised an urgent need of a direct and accurate measurement of force levels in the sub-micro-Newton range. Force measurements in the nano-Newton range are also essential in aerospace technology for the calibration of micropropulsion systems.[21] Nanomanipulation studies inside scanning electron microscopes (SEMs) have stimulated the design of special sample holders to couple the imaging and force probing system.[22–27] During these *in situ* SEM experiments, forces are usually estimated by measuring the elastic deflection of AFM cantilevers[22,23,25,27] or semiconductor nanowires.[28] The quantitative assessment of the deflections requires the use of SEM images, which frequently limits the force resolution due to pixel size. Moreover, this kind of nanomanipulation studies may be rather complex, because they frequently involve image acquisition at very different magnifications: (a) higher ones to observe small deflections on the cantilever (to compute force) and (b) lower ones allowing large field of view to observe the whole sample (strain assessment). Recently, direct force sensors based on the acquisition of electrical signals, exploiting microelectromechanical systems have been reported.[29,30] These sensors have been used to study the elongation and rupture of Carbon Nanotubes (CNTs), where the applied forces were in the 1–50 μN range and the obtained resolution was about 10–100 nN.[12,24,30,31]

Here, we describe the use of quartz TFs as direct and quantitative force sensor suitable for nanomanipulation experiments inside a SEM. Our approach is based on a simple and standard lock-in amplifier (LIA) setup, where an

a)Author to whom correspondence should be addressed. Electronic mail: oiko@ifi.unicamp.br

electrical signal from the TF resonance peak is used for the direct force evaluation. The TF response is initially calibrated against an AFM cantilever and, subsequently, the LIA signal alone allows the direct force value estimation. We have been able to directly measure forces in the 1–100 nN range with a resolution of a few nN during preliminary CNT mechanical deformation studies. We expect that this force resolution can be improved by additional experiments addressing accuracy issues during the sensor calibration.

II. DESCRIPTION OF THE EXPERIMENTAL SETUP

The quantitative TF-based force sensor described in this study follows the commonly applied procedure in AFM: a typical quartz tuning fork (Vishay Dale Electronics, Mod. XT38T) had a metallic probe tip affixed by non-conductive epoxy glue at the end of one of its prongs (leaving the other one free to oscillate, see Fig. 1). No charging effects were observed during the SEM experiments, regardless the use of a non-conductive epoxy. One can verify it from the electron microscopy images (Figs. 1(b) and 4(a)–4(d)) which do not present any characteristic features of charging (e.g., distortions or very bright spots). The probe tip was obtained through chemical etching/polishing of a tungsten wire (99.95% purity, 75 μm diameter, Advent Research Materials, Mod. W5588) applying the double lamellae drop-off technique.[32] We attached only one tip to the TF, leaving it unbalanced. Although it affects the TF signals, the quality of the resonance curves was still satisfactory for our purposes (quality factor of ∼10 000). The resonance frequency of the TF changes from its original value of (31763.3 ± 0.1) Hz to (31414.5 ± 0.5) Hz with the tip attachment and the quality factor in vacuum decreases from 47 000 to 10 000. Measurements in air were not performed once the whole experiment takes place inside the electron microscope's specimen chamber at 5.93×10^{-5} Pa.

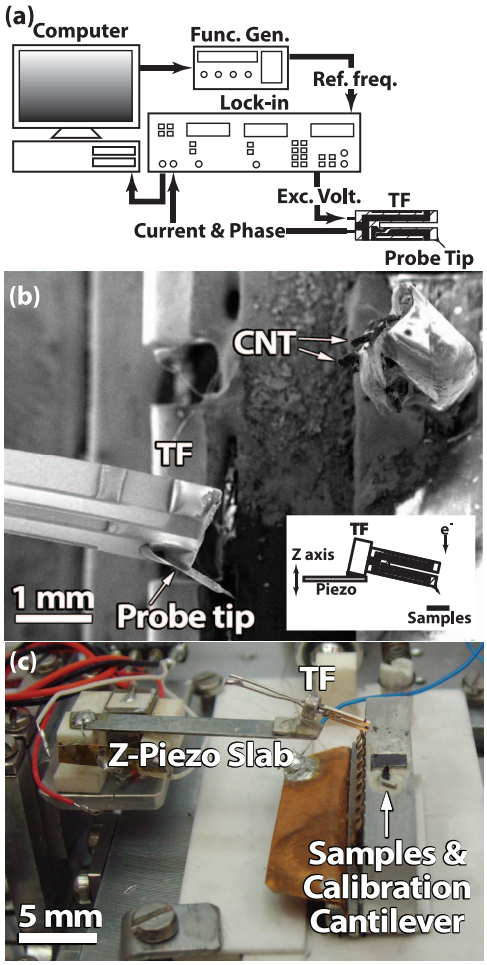

FIG. 1. (a) Experimental setup used for TF's excitation and signal acquisition, consisting of a computer, a function generator, a dual-phase lock-in amplifier, and the force sensor indicated by the TF with the probe tip (see text for explanations). (b) SEM image of the actual assembly of the TF with the probe tip and a scheme depicting its assembly on the nanomanipulator (inset). (c) Picture of the actual system with the TF mounted on the experimental setup.

The sensor's electronics consist of a function generator (Agilent 33250A) and a dual-phase LIA (Stanford Research Systems SR830 DSP) both controlled by a computer and operating in a similar fashion as described by Song[33] (see Fig. 1(a)). The LIA produces a sinusoidal signal as excitation voltage (marked as Exc. Volt. in Fig.1(a)) with amplitude of 4 mV_{rms} and frequency given by the function generator. It is also responsible for acquiring the TF's response, *i.e.*, its current's amplitude and phase with a precision of 5 pA and 1°, respectively. By varying the reference frequency on the function generator one is able to construct point-by-point the TF's resonance peak and the phase curve. The driven signal was kept as low as possible to minimize the prong's oscillation amplitudes and to guarantee that the resonator operates in the linear regime. The main concern regarding the TF amplitude of oscillation is the disturbance it may cause on the analyzed system. The reference frequency was swept in a 50 Hz window with steps of 0.5 Hz centered at the resonant frequency, and each curve was acquired in approximately 90 s, which is equivalent to 0.9 s per point. Considering that Q actually represents the number of cycles required for the TF to stabilize, we can deduce that it takes approximately $\Delta t \sim 0.32$ s for the system to self-stabilize ($\Delta t = Q\ T$, *where T is the TF period,* $1/f_{TF}$). Since this time is shorter than the one needed to acquire one single measurement, we may deduce that no transient effects appear even at the first acquired point of the TF resonance peak. Examples of the acquired signals and how they vary as a function of applied forces are described in detail in Sec. III.

It must be emphasized that the electronics setup represents one of the simplest ways to work with TFs. Comparing the aforementioned electronics with those required, for example, to apply directly the FM-AFM method,[7] a significant difference concerning complexity and cost can be easily deduced, although the FM-AFM setup allows other measurement modes not covered by the considered electronics. It is important to keep in mind that AFM is a scanning imaging microscopy, and it is essential to minimize dwell time per pixel. In contrast, speed is not a requirement in our rather complex and time-consuming *in situ* SEM manipulation experiments, so we can deal with an acquisition time of 90 s per force measurement point.

The TF sensor was tested using a homemade nanomanipulation sample-holder,[34] operating in an open-loop

configuration developed for *in situ* experiments inside a high resolution field-emission electron microscope (FEG-SEM, JEOL 6330F). The manipulator movement system is composed of two independent systems, one for coarse movement, based on picomotors (New Focus—Mod. 8321-UHV), and other for fine movements, based on piezo slabs and actuators. The former is characterized by a resolution of 20 nm on the X-axis and 30 nm on the Y-axis with total range of 5 mm and 15 mm, respectively. Z-axis calibration was not performed due to the SEM depth of focus. The latter has a resolution of 0.8 nm on the X-axis and 5 nm on the Y-axis, and a total range of 4 μm and 17 μm, respectively.[34] Fig. 1(b) displays a low-magnification SEM image of the TF on the manipulation stage. A scheme (Fig. 1(b), inset) and an actual picture (Fig. 1(c)) of the TF's assembly on the nanomanipulator are provided for reference. The TF is mounted on a piezo slab responsible for the fine movement on the Z-axis. Another important characteristic is that the samples and the calibration cantilever are both mounted on the nanomanipulator sample holder, which allows for the calibration and the manipulation experiments to be performed without removing the whole setup from the microscope chamber. This is of fundamental importance, in order to minimize external interferences and contaminations that may lead to changes on the TF's characteristics.

The setup orientation relative to the electron beam of the microscope is also indicated (Fig. 1(b), inset), and it turns out to be a fundamental characteristic for defining the force sensor design for *in situ* SEM experiments. As shown in Figs. 1(a) and 1(b), the probe tip is attached to the TF prong with an angle, not following the traditional normal mode or shear mode designs. There are two reasons for such a choice. First, it is essential to avoid the tip being hidden from the SEM electron beam by the TF prongs. Second, this geometrical configuration is necessary to assure that the tip will contact the sample before the prong does. Despite our efforts to keep the TF as parallel as possible to the cantilever, some misalignment is expected, once the sensor is manually assembled on the nanomanipulator. For the correct analysis of their contribution to the force quantification, such angles should be precisely measured; making a simple geometrical force vector projection, a misalignment of the order of 10°–20° would imply an error of ~5% in the measured force absolute value. To prevent electric interference and further propagation of electric noise, all the equipment including the microscope specimen chamber, polar piece, and the sample-holder were wired to the same ground potential.

III. SENSOR CALIBRATION AND CHARACTERIZATION

To develop a quantitative force sensor we must first analyze how the TF current amplitude and phase change when a force is applied on the probe tip. For this purpose, we have used the nanomanipulator to deflect an AFM cantilever by pressing on it, while the TF signals were monitored by the LIA. We observed that the resonance peak evolves monotonically with increasing force: peak amplitude is reduced and phase's minimum is raised (see Fig. 2(a)).

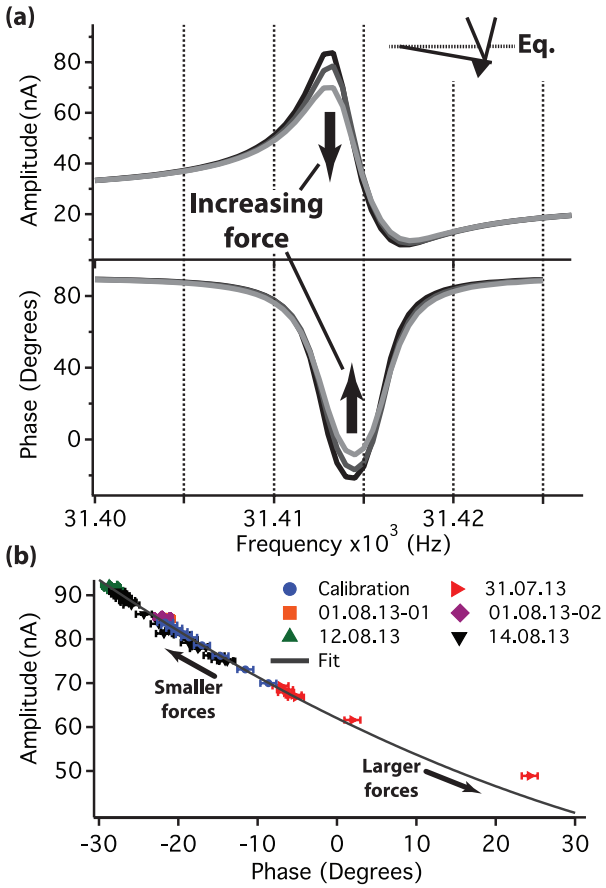

FIG. 2. (a) TF experimental curves acquired during *in situ* experiments for a progressively deflected Si AFM cantilever. Inset: experimental procedure used to analyze the TF's response to an external force. As the force is increased, the amplitude and phase shift of the resonance peak varies monotonically (amplitude is reduced and phase augmented, indicated by the arrows). (b) Scatter plot of resonance amplitude (A) and phase shift (P) obtained from different experiments realized with the same TF within a several week period. The solid line is a second order polynomial fit to the points generated during a quantitative force calibration experiment.

In order to correlate amplitude and/or phase with the applied force value we have carried out a calibration step where an AFM cantilever previously calibrated (following the method proposed by Sader,[35,36] elastic constant equal to 4.3 $\pm$ 0.3 $\times$ 10^{-2} N/m, CSG01-NT-MDT) was progressively deflected by pressing with the probe tip. The force values (F) were calculated using Hooke's law and measuring the cantilever deflection from SEM images. The amplitude maximum (A) and phase minimum (P) at resonance peak were obtained through interpolation of the experimental acquired data points. We have observed that the variations in the amplitude and phase as a function of force are indeed correlated (see Fig. 2(b)); then, it is not necessary to use both signals (A and P) to derive the applied force. In these terms, a calibration curve can be constructed just by linking the force to the amplitude maximum A (Fig. 3(a)). At this point, it is important to mention that our analysis has neglected any effect of the tip being attached with an angle relative to the TF's prong. The calibration curve is built using the total force, instead of decomposing it in parallel and normal components. We have taken care to minimize possible influence of torsional

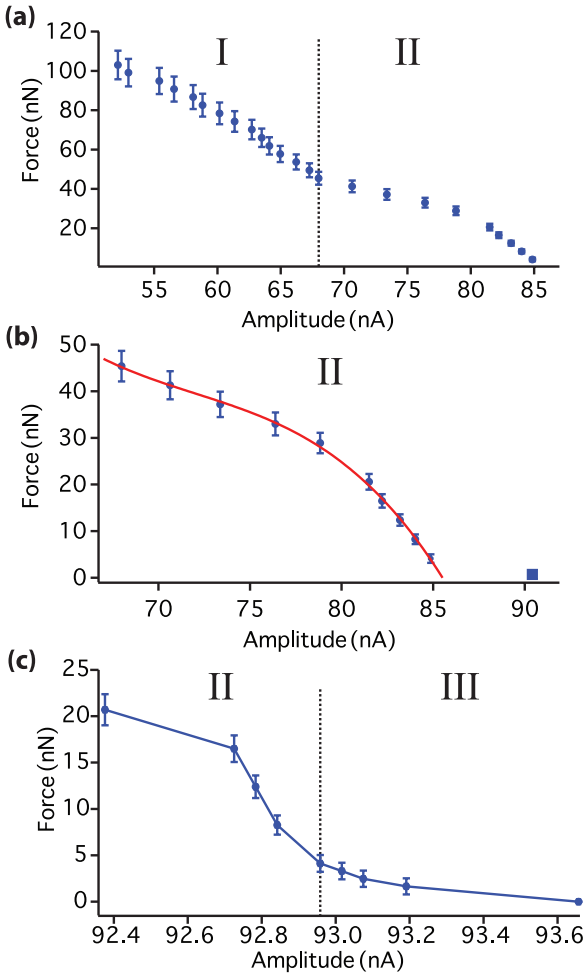

FIG. 3. (a) Applied force variation as a function of TF's maximum current at the resonance. The curve has been divided in two different regions due to abrupt changes in the slope at ∼40 nN force. (b) Close view of region II where the zero force point is included (square dot for an amplitude above 90 nA). The solid line corresponds to a third degree polynomial fit, which is used as conversion rule from the TF's signal to the force in further experiments. (c) Similar calibration experiment results obtained from a different TF where points in the region below 4 nN (region III) are acquired (see text for explanations). The line connecting the data points serves just as a guide for visualization.

components at the calibration cantilever during the calibration step. We have chosen to place the contact point between the probe tip and the AFM cantilever at the center of the pyramidal apex base, instead of at the edge of the cantilever. Although these efforts have been taken, some torsional components may still be present during the calibration acquisition.

The calibration curve can be divided in two distinct parts due to an abrupt change of behavior, characterized by the alteration of the slope of the curve at a force value of (45 ± 3) nN (in Figure 3(a) these different force regions were noted I and II). We have analyzed different TF sensors, and all of them displayed a change of slope for a force value in the 30–70 nN range. We attribute this behavior change to the activation of novel deformation mechanisms in the sensor, possibly at the W tip or its fixation region (glue). As for the W probe tips, it has been reported that during nanomanipulation experiments, very small W tips are easily bent when pressed against the sample or substrate.[34] In this sense, it is known that nanoscale metal rods may display mechanical properties quite different from their bulk behavior. For example, strengthening or softening has been reported depending on several geometrical factors (external size vs. grains size, etc.).[37–41] Studies exploring the size-effect in monocrystalline tungsten nanopillars have shown that for nanopillars with diameters ranging from 200 nm to 900 nm, the flow stress shows a clear size effect.[40] If we model our tips as cylinders with diameter around 100 nm, we should expect plastic deformation for forces in the tens of micro-Newton range.[38] To check this point, we have also prepared a TF force sensor with the pristine W wire (without the sharp tip electrochemical preparation procedure), and the force calibration curve also showed a slope change around 40 nN. Briefly, the slope change in the calibration curves cannot be accounted by the mechanical deformation of the probe tip. Further experiments are in progress to understand if this slope change is associated with the W wire fixing point, in particular addressing the gluing procedure and the glue quality.

The plot relating applied force and amplitude (Fig. 3(b)) clearly indicates that zero force point is in a position quite different from the tendency followed by the other experimental points in the 5–20 nN range. A detailed measurement of a TF sensor response in the smaller forces regime (0–20 nN force range) is displayed in Fig. 3(c) (note that a different TF sensor has been used for this experiment). This graphic is divided in two distinct regions around 4 nN, II and III. Although the experimental points in Region III display a different behavior, they evolve very smoothly and, in a well-behaved manner, even for forces ≤1 nN, following a smooth curve that would extrapolate into the zero force experimental point. This defines a third TF response region (III), corresponding to lower force values (0–3 nN).

A natural question arises, why the TF response change for lower forces during this calibration procedure? In fact, the system can be described as a forced oscillator, where the TF induces by compression a forced oscillation in the AFM cantilever. Then we must analyze if the contact regime (coupling) between the probe tip and the cantilever is well defined for such low forces. Using the experimental parameters (TF resonance frequency, quality factor, excitation voltage, and electric current at the resonance), it is possible to calculate the TF oscillation amplitude, a_{TF}, as (21 ± 1) nm.[42] First, this a_{TF} value corresponds to the expected static cantilever displacement (Δx) when the applied force is ∼1 nN; this certainly represents an intrinsic source of uncertainty for quantitative force determination. Second, the AFM cantilever is much softer than the TF, its resonant frequency ($f_{CL} \sim 12$ kHz) is much lower than the TF one ($f_{TF} \sim 32$ kHz). Hence, in order to keep the TF-cantilever mechanical contact during a compressive experiment, it would be necessary that the cantilever be able to follow properly the TF oscillation. From a simply dynamical point of view, this means that the TF and cantilever maximal acceleration amplitudes (α) must be comparable. From the harmonic oscillator theory we have that α is given by $a_0\omega^2$, where a_0 is the oscillation amplitude and ω is the frequency in radians ($\omega = 2\pi f$). Then, for an oscillation of amplitude a_{TF}, we can obtain that α_{TF} is (846 ± 5) m/s^2, while for the cantilever α_{CL} is (121 ± 5) m/s^2. As α_{CL}

$< \alpha_{TF}$, it is clear that the cantilever cannot follow the TF oscillations properly for lower forces ($\Delta x \sim a_0$), and the contact between them is intermittent. As a consequence, the TF oscillation is weakly modified and the sensor response is very low, explaining the different TF electrical response in Region III, Fig. 3(c)). In contrast, for conditions where $\Delta x > a_{TF}$, the TF resonant peak shows clear and easily detectable changes. To overcome this difficulty and extend the TF force sensing working region to lower forces, it is possible to diminish a_{TF} by modifying the TF's excitation for example.

In order to explore the use of TF as quantitative force sensor, we will restrict our study to analyze applied forces with values in the 5 to 40 nN range (see Fig. 3(a), region marked II). In this way, we avoid the slope change above 40 nN, and also the lower force region (0–3 nN), where the errors are rather high (30%–60%). The experimental points (*F vs. A*) in region II (Fig. 3(b)) are distributed as following a very well behaved function. In this figure, the solid line is a third-degree polynomial fit that will be applied as conversion function *g* to calculate the force value as $F = g(A)$. With the calibrated response function *g(A)* in hands, it is possible then to use the force sensor in experiments of mechanical deformation and obtain, directly from the TF's amplitude solely, the applied force. It is important to emphasize that, after the calibration step, the force quantification has become completely independent of SEM images taken during the nanomanipulation experiment. This not only generates an improvement on the obtained force resolution, but also significantly simplifies the experimental studies, reducing electron irradiation dose, and the possible deposition of amorphous carbon contamination on the analyzed samples. The force error bar is mainly related by the quality of the fitting and accuracy error related with the calibration procedure.

We must analyze the reproducibility and reliability of the TF sensor. Therefore, we have plotted on the same graphic the *A vs. P* obtained from many different experiments (including calibration step and several nanomanipulation studies) using the same force sensor during a several week period (Fig. 2(b)). It is clear that the relation between phase and amplitude is a very well behaved phenomenon. The solid curve corresponds to a second-degree polynomial fit adjusted only to the quantitative force calibration experiment. The agreement found between the fit and the other experimental points is remarkably impressive. It is important to mention that the calibration curve varies from sensor to sensor; then the *F* vs. *A* calibration curve must be performed for each TF before use. Since small changes in the sensor's preparation and also on the environment where the experiment is conducted are common, *i.e.*, variations on the amount of glue applied or the length of the wire from where the tip is etched, changes in the electromagnetic background noise, temperature fluctuations, etc., it is required to calibrate the sensor before any experiment. Our nanomanipulation sample holder may fit several samples and we keep one or two slots for AFM cantilevers to be used for the initial calibration of the TF quantitative force sensor.

Once we have calibrated and tested the sensor for measuring compression forces (Fig. 3), it is essential to evaluate the TFs response when the probe tip is submitted to a tensile force instead of compression. Although from symmetry arguments one may expect that in first approach both situations have similar response, an experimental proof is still required. Hence, we decided to realize experiments where the TF probe tip was attached (glued) to the AFM cantilever end; then the cantilever was deflected in both directions (pushing and pulling). This ideal experiment turned out to be actually rather complex, because we had to glue the tip under an optical microscope and, subsequently, install the nanomanipulator inside the microscope. These several steps handling of the system lead to the AFM cantilever rupture. Then, we were forced to make the whole experiment in air under the optical microscope, what changed the TF resonance response due to the different environment (mainly change in pressure/vacuum condition). In an attempt to make a more stringent verification of the sensor's reproducibility, the experiment was carried out according to the following procedure: the probe tip was displaced by a predetermined amount pushing the cantilever and the TF's signal was recorded. Then the cantilever was brought to its equilibrium position and pulled by the same amount that it had been previously deflected and the TF's signal was then recorded. This procedure was repeated for different force values, keeping always the alternation of pushing and pulling forces. The TF signals were acquired with the same procedure, but the AFM cantilever deflection was measured by analyzing the TF base displacement (the TF is much stiffer than the AFM cantilever). The TF support was driven by a linear Piezo micromotor;[34] counting the motor steps, we derived the support linear displacement. Table I displays the different forces measured for tension and compression and the corresponding TF signals. Although the experimental conditions were rather difficult, a very good agreement is observed indicating that the TF shows a symmetrical behavior.

TABLE I. Comparison of TF response to analyze compressive and tensile forces.

Force (±1 nN)	Compression Current (±0.1 nA)	Tension Current (±0.1 nA)
6	19.4	19.5
10	19.2	19.2
12	19.2	19.0
15	18.9	18.8

IV. APPLICATION AND PERFORMANCE

Once the force sensor has been properly calibrated and characterized, this section will address the sensor's application on measuring forces involved during the mechanical manipulation of multi-walled carbon nanotubes (MWCNT) bundles. The nanotubes were produced by arc discharge (20 V, 80 A) in He atmosphere (500 mbar) and are in average a few micrometers long.

Electron beam induced deposition of amorphous carbon (EBID) was used to attach the nanotubes at the W probe tip.[22,23] During the mechanical experiments we used a second EBID region deposited over the CNT surface as a reference point to easily observe displacement in the SEM images (indicated by an arrow in Fig. 4). The nanotube sample was

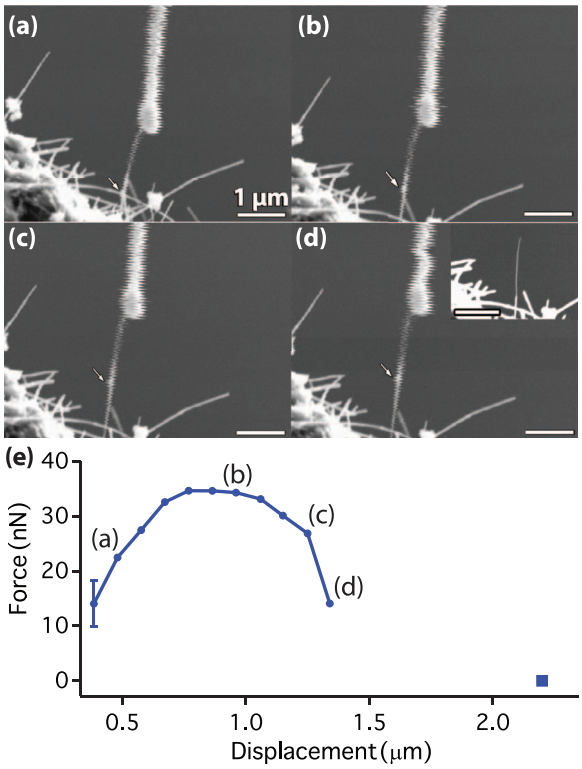

FIG. 4. ((a)–(d)) Sequence demonstrating an *in situ* manipulation experiment with MWCNT bundles where some CNTs are pulled away from the bundle. Inset: the remaining CNT after the pulling is completed (e). The scale bars correspond to 1 μm. Force measurements as a function of the CNT's displacement away from the tip. Values were obtained from the TF's signals and the calibration procedure described in the text (the square dot at the right indicates the zero force point).

repeatedly retracted from the probe tip by steps of (96 ± 20) nm (TF was kept fixed). Figs. 4(a)–4(d) show some large field of view images; Fig. 4(e) displays the measured forces as a function of elongation. The forces measured during this experiment were in the 14–35 nN range, and they were obtained from the TF electrical signal converted into forces using calibration curve from Fig. 3(b).

The experiment consisted of measuring the forces as some of the CNTs were extracted from the bundle. Due to technical constraints (mainly microscope resolution), it has not been possible to distinguish how many nanotubes were removed from the bundle and how many were left. In our experiments (see force vs. distance plot in Fig. 4(e)), we observe that when we start pulling the CNT bundle, the forces build up until a maximum value of ∼35 nN; it stays approximately constant (within the error bar) for about 300 nm, and starts to decrease until the bundle ruptures. The force values acquired in this study are in great accordance with values found in the already reported similar studies.[22,43–45] The force variation along the experiments is similar to that predicted by the theoretical work proposed by Wei *et al.*,[44] which described a force saturation in shear experiments pulling CNT bundles. These authors predicted that the shear force when sliding a CNT in a bundle should increase with the overlap length, and that a saturation of the shear force should be observed when the tubes overlap attains 300–400 nm. Our results also indicate that we had to perform a total displacement of ∼1 μm to attain the zero point force, measuring from the point where shear force start to decrease (the experiment has been done in a direction opposite to the theoretical explanation presented above). Although our experimental measurement is about twice the distance predicted by the theoretical model of Wei *et al.*,[44] we consider that the agreement is very good considering the approximations used in the model.

Due to the orientation of the glued probe tip in relation to the TF prongs, a deeper understanding requires further experimental and theoretical studies to evaluate the contributions of longitudinal and normal forces to the total force value used in this work. We are confident that once the sensor has been thoroughly calibrated with the procedure described here, the measured values are coherent and represent a very good quantitative estimation of the total force's magnitude applied in the experiment.

V. SUMMARY

We have described the development of a TF based force sensor for quantitative and direct measurement of applied forces during nanomanipulation experiments *in situ* in a SEM. The force sensor must be initially calibrated against a force standard and then the force estimation is based exclusively on the electric signals from the TF. This allows the decoupling of force measurements and SEM imaging during the manipulation experiments. We have been able to measure forces in the 5–45 nN range with a force resolution of few nN. The force sensor was applied for mechanical tests involving the tensile deformation of multi-walled carbon nanotubes' bundles. The derived results were in very good agreement with previously reported experiments.

The forces were quantified with an error bar of 3–4 nN; however, a quick look at the experimental points in Fig. 4(e) suggests these bar values seem to be somewhat overestimated. In fact, the experimental point dispersion is much lower than should be expected for such an error bar. In our study, one of the main sources of error in the force quantification is actually the accuracy, associated with the cantilever elastic constant that is used as force standard for the calibration curve. By reducing the error in the cantilever elastic constant from the current 7% to around 5% would already represent a 33% reduction in the final force error. Also, our calibration curve is based on a 3rd order polynomial fit model, which has been selected without any physical underlying model. More accurate models relating the TF signal with the applied force would also contribute substantially to improve the sensor sensitivity. We expect that with further work on the precision and accuracy of the calibration process and signal interpretation, the final force error would lie in the nN range.

ACKNOWLEDGMENTS

This work is supported by FAPESP (Fundação de Amparo à Pesquisa do Estado de São Paulo - Proc. No. 2010/51028-4) and CNPq (Conselho Nacional de Desenvolvimento Científico e Tecnológico - Proc. No. 476458/2011-0). The authors are grateful to Professor M. Cotta for providing the AFM cantilevers used in the experiments and to the

Laboratório Nacional de Nanotecnologia (LNNano) for allowing the use of their scanning electron microscope.

[1]See http://www.nano.gov/node/250 for further information; download the report at File Downloads and refer to Section 3, "Instrumentation and Metrology for Nanomechanics."
[2]M. R. Falvo, G. J. Clary, R. M. Taylor II, V. Chi, F. P. Brooks, Jr., S. Washburn, and R. Superfine, Nature **389**, 582 (1997).
[3]M. R. Falvo, R. M. Taylor II, A. Helser, V. Chi, F. P. Brooks, Jr., S. Washburn, and R. Superfine, Nature **397**, 236 (1999).
[4]T. W. Tombler, C. Zhou, L. Alexseyev, J. Kong, H. Dai, L. Liu, C. S. Jayanthi, M. Tang, and S.-Y. Wu, Nature **405**, 769 (2000).
[5]F. J. Giessibl, Phys. Rev. B **56**, 16010 (1997).
[6]R. García and R. Pérez, Surf. Sci. Rep. **47**, 197 (2002).
[7]J. C. Acosta, G. Hwang, J. Polesel-Maris, and S. Régnier, Rev. Sci. Instrum. **82**, 035116 (2011).
[8]F. J. Giessibl, Appl. Phys. Lett. **78**, 123 (2001).
[9]J. E. Sader and S. P. Jarvis, Appl. Phys. Lett. **84**, 1801 (2004).
[10]J. E. Sader, T. Uchihashi, M. J. Higgins, A. Farrell, Y. Nakayama, and S. P. Jarvis, Nanotechnology **16**, S94 (2005).
[11]M. Lee, J. Jahng, K. Kim, and W. Jhe, Appl. Phys. Lett. **91**, 023117 (2007).
[12]R. D. Grober, J. Acimovic, J. Schuck, D. Hessman, P. J. Kindlemann, J. Hespanha, A. S. Morse, K. Karrai, I. Tiemann, and S. Manus, Rev. Sci. Instrum. **71**, 2776 (2000).
[13]Y. Qin and R. Reifenberger, Rev. Sci. Instrum. **78**, 063704 (2007).
[14]F. J. Giessibl, S. Hembacher, H. Bielefeldt, and J. Mannhart, Science **289**, 422 (2000).
[15]F. J. Giessibl, Rev. Mod. Phys. **75**, 949 (2003).
[16]J. Jersch, T. Maletzky, and H. Fuchs, Rev. Sci. Instrum. **77**, 083701 (2006).
[17]M. Ferrara, Nanotechnology **14**, 427 (2003).
[18]A. J. Weymouth, D. Meuer, P. Mutombo, T. Wutscher, M. Ondracek, P. Jelinek, and F. J. Giessibl, Phys. Rev. Lett. **111**, 126103 (2013).
[19]K. Kapoor, V. Kanawade, V. Shukla, and S. Patil, Rev. Sci. Instrum. **84**, 025101 (2013).
[20]L. M. Dorogin, S. Vlassov, B. Polyakov, M. Antsov, R. Lõhmus, I. Kink, and A. E. Romanov, Phys. Status Solidi B **250**, 305 (2013).
[21]J. Mueller, *Micropropulsion for Small Spacecraft, Progress in Astronautics and Aeronautics*, edited by M. Micci and A. Ketsdever (AIAA, Reston, VA, 2000), Vol. 187, pp. 45–137.
[22]M.-F. Yu, O. Lourie, M. J. Dyer, K. Moloni, T. F. Kelly, and R. S. Ruoff, Science **287**, 637 (2000).
[23]X. Chen, S. Zhang, D. A. Dikin, W. Ding, R. S. Ruoff, L. Pan, and Y. Nakayama, Nano Lett. **3**, 1299 (2003).
[24]W. Ding, L. Calabri, K. M. Kohlhaas, J. Chen, D. A. Dikin, and R. S. Ruoff, Exp. Mech. **47**, 25 (2007).
[25]J. Zang, L. Bao, R. A. Webb, and X. Li, Nano Lett. **11**, 4885 (2011).
[26]S. Y. Ryu, J. Xiao, W. I. Park, K. S. Son, Y. Y. Huang, U. Paik, and J. A. Rogers, Nano Lett. **9**, 3214 (2009).
[27]W. Rong, W. Ding, L. Mädler, R. S. Ruoff, and S. K. Friedlander, Nano Lett. **6**, 2646 (2006).
[28]R. Zhang, Z. Ning, Y. Zhang, Q. Zheng, Q. Chen, H. Xie, Q. Zhang, W. Qian, and F. Wei, Nat. Nanotechnol. **8**, 912 (2013).
[29]Y. Zhu, N. Moldovan, and H. D. Espinosa, Appl. Phys. Lett. **86**, 013506 (2005).
[30]B. Peng, M. Locascio, P. Zapol, S. Li, S. L. Mielke, G. C. Schatz, and H. D. Espinosa, Nat. Nanotechnol. **3**, 626 (2008).
[31]S. Lu, Z. Guo, W. Ding, and R. S. Ruoff, Rev. Sci. Instrum. **77**, 056103 (2006).
[32]M. Kulawik, M. Nowicki, G. Thielsch, L. Cramer, H.-P. Rust, H.-J. Freund, T. P. Pearl, and P. S. Weiss, Rev. Sci. Instrum. **74**, 1027 (2003).
[33]S.-H. Song, Rev. Sci. Instrum. **80**, 034703 (2009).
[34]D. Nakabayashi, P. C. Silva, J. C. González, V. Rodrigues, and D. Ugarte, Microsc. Microanal. **12**, 311 (2006).
[35]J. E. Sader, J. Appl. Phys. **84**(1), 64 (1998).
[36]J. E. Sader, *et al.*, Rev. Sci. Instrum. **70**(10), 3967 (1999).
[37]M. D. Uchic, D. M. Dimiduk, J. N. Florando, and W. D. Nix, Science **305**, 986 (2004).
[38]S. Brinckmann, J.-Y. Kim, and J. Greer, Phys. Rev. Lett. **100**, 155502 (2008).
[39]D. Jang, X. Li, H. Gao, and J. Greer, Nat. Nanotechnol. **7**, 594 (2012).
[40]J.-Y. Kim, D. Jang, and J. R. Greer, Acta Mater. **58**, 2355 (2010).
[41]D. Jang and J. R. Greer, Scr. Mater. **64**, 77 (2011).
[42]J. Liu, A. Callegari, M. Stark, and M. Chergui, Ultramicroscopy **109**, 81 (2008).
[43]M.-F. Yu, B. I. Yakobson, and R. S. Ruoff, J. Phys. Chem. B **104**, 8764 (2000).
[44]X. Wei, M. Naraghi, and H. D. Espinosa, ACS Nano **6**, 2333 (2012).
[45]Q. Zheng, J. Z. Liu, and Q. Jiang, Phys. Rev. B **65**, 245409 (2002).